Kinetic Study of the CCl_2 Radical Recombination Reaction by Laser-Induced Fluorescence Technique

NICOLÁS D. GÓMEZ,[1] VIOLETA D'ACCURSO,[1] V. MARIANA FREYTES,[2] FRANCISCO A. MANZANO,[1] JORGE CODNIA,[1] M. LAURA AZCÁRATE[1,2]

[1]DEILAP (CITEDEF), *Buenos Aires* B1603ALO, *Argentina*

[2]*Carrera del Investigador* (CONICET), *Buenos Aires, Argentina*

Received 12 January 2012; revised 10 August 2012; 19 October 2012; 22 October 2012; accepted 23 October 2012

DOI 10.1002/kin.20766
Published online 26 March 2013 in Wiley Online Library (wileyonlinelibrary.com).

ABSTRACT: An experimental setup that coupled IR multiple-photon dissociation (IRMPD) and laser-induced fluorescence (LIF) techniques was implemented to study the kinetics of the recombination reaction of dichlorocarbene radicals, CCl_2, in an Ar bath. The CCl_2 radicals were generated by IRMPD of $CDCl_3$. The time dependence of the CCl_2 radicals' concentration in the presence of Ar was determined by LIF. The experimental conditions achieved allowed us to associate the decrease in the concentration of radicals to the self-recombination reaction to form C_2Cl_4. The rate constant for this reaction was determined in both the falloff and the high-pressure regimes at room temperature. The values obtained were $k_0 = (2.23 \pm 0.89) \times 10^{-29}$ cm^6 molecules^{-2} s^{-1} and $k_\infty = (6.73 \pm 0.23) \times 10^{-13}$ cm^3 molecules^{-1} s^{-1}, respectively. © 2013 Wiley Periodicals, Inc. Int J Chem Kinet 45: 306–313, 2013

INTRODUCTION

Hazardous waste treatment is an issue of major concern. Among the various types of hazardous waste, chlorinated hydrocarbons are produced in many industries. Chlorinated compounds in commercial use include pesticides, pharmaceuticals, disinfectants, and consumer products such as plastics. Chlorinated hydrocarbons are used as intermediates in the synthesis of other chemicals as well as to produce silicon for electronic chips and epoxy resins. Chlorinated methanes, ethanes, and ethenes solvents are used for degreasing and dry cleaning. Polychlorinated biphenyls and triphenyls are used as dielectric and coolant fluids in transformers, capacitors, and electric motors. Thus, there is a great need to destroy huge quantities of chlorinated hydrocarbons. Two processes are mainly employed for the treatment of these types of waste: incineration and pyrolysis. Alternative chemical degradation techniques such as UV/ozonation, semiconductor photocatalysis, and catalytic destruction of chlorocarbons with steam are currently under research [1–6]. The pyrolysis and

Correspondence to: M. Laura Azcárate; e-mail: lazcarate@citedef.gob.ar.

Contract grant sponsor: Consejo Nacional de Investigaciones Científicas y Técnicas (CONICET) of Argentina.
Contract grant number: 1220100100425.

combustion of chlorinated hydrocarbons also leads to the formation of chlorinated aromatic species [7]. It is therefore of great interest to understand the elementary reaction mechanisms involved in these processes as well as to determine their rate constants in view to optimize chlorinated hydrocarbon destruction.

Particularly, one of the halogenated hydrocarbons widely used in industry is chloroform. Large amounts of this compound are produced annually since its main use is as a precursor to Teflon. It is also used as a solvent in the pharmaceutical, dye, pesticide, and dry cleaning industries. Pyrolysis of chloroform under a broad range of conditions has been extensively studied in the past few decades [7–21]. Reaction pathways to give account of the products determined at different stages of the reaction have been described. Earlier studies proposed C–Cl fission (1a) as the main primary dissociation step [8–10]. Later investigations have concluded that the three-center HCl elimination reaction (1b) is the dominant initiation step [11,14,15,17–21]:

$$CHCl_3 \rightarrow CCl_2H + Cl \quad (1a)$$

$$\rightarrow CCl_2 + HCl \quad (1b)$$

More specifically, the infrared multiple-photon dissociation (IRMPD) of $CDCl_3$ with a TEA CO_2 laser occurs only through channel (1b) with no further fragmentation of the CCl_2 radical [11,22].

In the above-mentioned chloroform pyrolysis studies, C_2Cl_4 has been the major intermediate chlorocarbon product detected over a wide temperature range [9]. The main pathway proposed to C_2Cl_4 formation is the combination reaction of two dichlorocarbene radicals, CCl_2 [15,18,20], (2). Other pathways include the insertion reaction of CCl_2 radical with $CHCl_3$ [15,20], (3), and the combination reactions of CCl_3 (formed in the Cl abstraction of H from $CHCl_3$) with CCl_2 [15,18,20] and $CHCl_2$ [15], (4) and (5), respectively:

$$CCl_2 + CCl_2 \rightarrow C_2Cl_4 \quad (2)$$

$$CCl_2 + CHCl_3 \rightarrow C_2Cl_4 + HCl \quad (3)$$

$$CCl_2 + CCl_3 \rightarrow C_2Cl_4 + Cl \quad (4)$$

$$CCl_3 + CHCl_2 \rightarrow C_2Cl_4 + HCl \quad (5)$$

The recombination reaction of dichlorocarbene radicals to form C_2Cl_4 has been scarcely studied. Won and Bozzelli [15] studied the pyrolysis of $CHCl_3$ in a reaction system consisting of 1% $CHCl_3$ in 760 Torr Ar in the temperature range of 800–1073 K. Gas chromatographic analysis was used to determine the reactant and products concentrations as a function of temperature at different reaction times. They proposed a detailed kinetic reaction mechanism consisting of 31 species and 67 elementary reactions to describe the reactant loss and the product formation, up to C_2 compounds. The mechanism describes the overall reaction process quite well but overestimates the C_2Cl_4 concentrations over the temperature range of 848–953 K. The high-pressure limit rate constant for the CCl_2 recombination reaction to form C_2Cl_4 calculated using unimolecular quantum version of Rice–Ramsperger–Kassel (QRRK) theory was 1.1×10^{-12} exp(2.5 kcal/mol/*RT*) cm^3 $molecules^{-1}$ s^{-1}.

Kumaran et al. [18] studied the pyrolysis of 1% and 4% $CHCl_3$ in Kr between 1282 and 1878 K. They used the laser schlieren technique to measure $CHCl_3$ decomposition, and time-resolved Cl formation was followed by the Cl-atom resonance absorption spectroscopic technique. A kinetic reaction mechanism consisting of six elementary reactions was used to describe the secondary CCl_2 chemistry. They reported a termolecular rate constant for the CCl_2 recombination reaction to form C_2Cl_4 in the falloff region derived with this mechanism of 1.6×10^{-32} exp(5.9 kcal/mol/*RT*) cm^6 $molecules^{-2}$ s^{-1}.

In 2003, Zhu and Bozzelli [20] analyzed previous literature results of the thermal conversion of $CHCl_3$ to CCl_4 in the presence of Cl_2 in the 846–908 K temperature range using a detailed mechanism that included 38 elementary reactions. The high-pressure limit rate constant for the association reaction of two CCl_2 radicals to form C_2Cl_4, which resulted from their QRRK-master equation calculations, was 4.5×10^{30} $T^{-14.2}$ exp(–9.2 kcal/mol/*RT*) cm^3 $molecules^{-1}$ s^{-1}.

In the above-mentioned works, the rate constant for the recombination reaction of two CCl_2 radicals to form C_2Cl_4 was calculated from complex mechanisms used to fit products distributions from $CHCl_3$ pyrolysis, employing Rice–Ramsperger–Kassel–Marcus (RRKM) and QRRK rate theories.

In this work, we have used laser-induced fluorescence (LIF) supported by Fourier transform IR spectrometry (FTIR) to study the CCl_2 association reaction to form C_2Cl_4 in an Ar bath. The LIF technique employed has allowed us to considerably simplify the reaction mechanism and to determine the rate constant in a direct manner. The CCl_2 radicals were generated by IRMPD of $CDCl_3$ and then excited in the transition $A^1B_1(0,4,0) \leftarrow X^1A_1(0,0,0)$. The time-dependent radical concentration was evaluated from the intensity of the fluorescence emitted by the excited species as they returned to the electronic ground state, which was detected for different delay times between the dissociation and the excitation pulses. The particular irradiation and LIF detection system's geometry

used ensured that the LIF signal detected is related to the fraction of molecules dissociated per pulse in a region of constant fluence [22]. Since the fluence value in the intersection zone of the observation and the dissociation volumes corresponded to the dissociation saturation value, every $CDCl_3$ molecule in this region was dissociated through the three-center DCl elimination pathway (1b) [22]. Thus, the time dependence of the CCl_2 radical concentration can be directly associated to the recombination reaction to form C_2Cl_4 (2). The rate constant for this reaction was determined in both the falloff and the high-pressure regimes.

EXPERIMENTAL

The time dependence of the CCl_2 radical concentration generated in the IRMPD of $CDCl_3$ was determined coupling IRMPD and LIF techniques. The experimental setup shown in Fig. 1 was described in detail elsewhere [22,23]. Briefly, the IRMPD of $CDCl_3$ was implemented using a multimode, pulsed TEA CO_2 laser with a repetition rate of 1 Hz tuned to the 10P(48) emission line. The laser radiation was focused into the center of the reaction cell with a 9.4 cm focal length ZnSe lens determining a beam's spot diameter at the focus and a Rayleigh range of 0.74 and 3.6 mm, respectively.

The radicals were electronically excited with a dye laser pumped by a frequency-tripled Nd:YAG laser pulsed at a repetition rate of 10 Hz. The dye laser consisted of an oscillatory stage followed by an amplification stage. The dye used was Coumarin 540 (Exciton), and the laser wavelength, controlled by an Avantes spectrometer, Ava Spec 3648, was tuned to 541 nm resonant with the CCl_2 electronic transition $A^1B_1(0,4,0) \leftarrow X^1A_1(0,0,0)$.

The laser beams entered the reaction cell collinearly, and the fluorescence signal was detected at 90° as shown in Fig. 1. A photomultiplier tube, RCA 1P28, was used for the detection of the fluorescence signal and a long-pass interference filter and an iris were disposed at the entrance of the photomultiplier tube. To increase the solid angle of detection, part of the fluorescence emitted by the CCl_2 radicals was directed to the photomultiplier tube by a two-lens system (10 and 24 cm focal lengths, respectively). The iris aperture was fixed so as to obtain an observation volume coincident with the volume in which the probability of dissociation is equal to one.

The Nd:YAG and TEA CO_2 lasers emissions were externally controlled with a Stanford Research Systems delay unit, DG 535. One channel of the delay unit was used to trigger the TEA CO_2 laser. As shown in Fig. 1, the output of this channel was connected to the entrance of a frequency divider so as to obtain a repetition rate of 1 Hz. Another channel was used to trigger the Nd:YAG laser. The Nd:YAG laser trigger was delayed with respect to that of the TEA CO_2 laser. The dye and TEA CO_2 lasers' output energies, 200 μJ and 1 J, respectively, were monitored from the beam reflections on different beam-splitters and registered by two GenTec meters. In all the experiments, the TEA CO_2 laser fluence at the beam waist was 100 J cm^{-2}. The fluorescence signals for different delay times as well as the pulse-to-pulse TEA CO_2 and dye lasers' output energies were acquired with an oscilloscope, Tektronix DPO 7054.

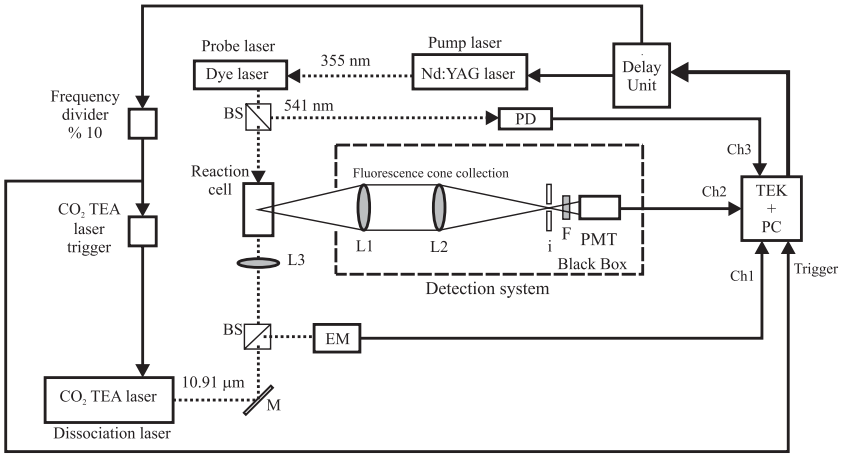

Figure 1 Experimental setup scheme. EM: energy meter, L1, L2: quartz lenses, L3: ZnSe lens, BS: beam-splitters, TEK: digital oscilloscope with incorporated PC, PMT: photomultiplier, F: filter, i: iris, PD: photodiode, M: mirror.

The delay times were varied in a geometric progression between 1 μs and 10 ms so as to characterize processes that occur in different timescales with the same resolution. In addition, to eliminate history effects, the delay times of each series of experiments were chosen at random. A specific program was developed for the control of the whole experiment by a PC.

The samples of $CDCl_3$ (Merck; 99.98%) and Ar (Alphagas; 99.9995%) were prepared in a high vacuum system, consisting of a turbomolecular pump (Leybold, Turbovac) pumped by a rotary vane pump (Leybold, Trivac) and introduced in a cylindrical static Pyrex glass cell 3 cm in diameter and 10 cm long. The partial pressures of the reactant and products were controlled by FTIR spectrometry. In all experiments, the $CDCl_3$ pressure was fixed at 1 Torr and the Ar pressure was varied in the 0–30 Torr range. To consider that the CCl_2 concentration produced in each pulse was constant, the global dissociation was kept less than 10%.

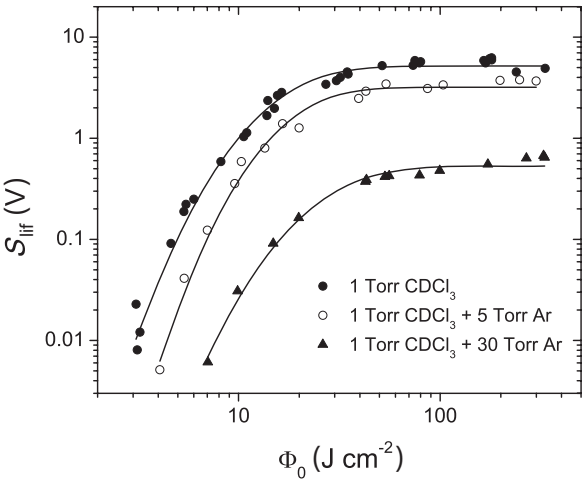

Figure 2 Fluence dependence of the LIF signal for mixtures of 1 Torr $CDCl_3$ with Ar.

RESULTS

The LIF signal is characterized by a fast rise time due to the fluorescence emission produced in the electronic decay to the ground state followed by a slow decay given by the detection system response. The LIF signal peak amplitude, S_{lif}, was used as an estimator of the fluorescence intensity and, therefore, of the CCl_2 concentration.

To understand both the formation and the kinetic mechanisms of the CCl_2 radicals, we will first describe some results concerning IRMPD of $CDCl_3$ obtained in previous works [22,23] with the same experimental setup. We have implemented a LIF technique, which allowed monitoring the fluence dependence of the CCl_2 radicals generated in the IRMPD of $CDCl_3$ in pure samples [22] and in mixtures with Ar [23]. Figure 2 shows the results obtained for a sample of 1 Torr of pure $CDCl_3$ and in mixtures with 5 and 30 Torr of Ar. The three curves are characterized by two well-differentiated regimes. In the 1–40 J/cm^2 range, the LIF signal increases with increasing fluence and then it reaches a plateau corresponding to the saturation regime. The fluence value for which saturation is attained depends on the Ar pressure and ranges between 20 and 30 J cm^{-2} for Ar pressures varying between 0 and 30 Torr. It can be observed that as the Ar pressure is increased, the LIF signal saturation value decreases due to collisional quenching of the excited CCl_2 radicals. Since on the one hand the dye laser is tuned resonantly with the electronic transition $A^1B_1(0,4,0) \leftarrow X^1A_1(0,0,0)$ of the CCl_2 radicals and, on the other hand, at 100 J cm^{-2} the fluorescence signal has reached a saturation regime for all Ar pressures, one can infer that every $CDCl_3$ molecule in the observation volume is dissociated through the three-center DCl elimination reaction (1b).

Therefore, during the acquisition time, the observation volume will only contain CCl_2 radicals, DCl, C_2Cl_4, and Ar so that the contribution of the insertion reaction of CCl_2 radical with $CDCl_3$ (3) to the CCl_2 radicals disappearance observed would be negligible. Contributions of the combination reactions of CCl_3 with CCl_2 (4) and $CHCl_2$ (5), respectively, can also be discarded since the CCl_3 radicals are mainly formed in the Cl abstraction of H from $CHCl_3$ [15,18,20], which does not take place in our experimental conditions. Thus, in our experimental conditions, the reaction mechanism following $CDCl_3$ IRMPD can be reduced to the occurrence of reaction (2).

In addition, we have used FTIR spectrometry to determine the final products in the irradiated samples. In accordance with the above considerations, these spectra showed that the major products obtained were DCl and C_2Cl_4 and that CCl_4 was the only minor product. CCl_4 is assumed to be formed in secondary chemistry occurring out of the observation volume.

To study the CCl_2 radicals reactions, we have varied the delay between the dissociation and excitation lasers in the range 1 μs–10 ms. A typical curve showing the dependence of the fluorescence signal maximum on the laser pulses' delay time for an Ar pressure of 25 Torr and a fluence of 100 J/cm^2 is shown in Fig. 3. Owing to the large time range used, the delay time is shown in a logarithmic scale.

Taking into account that the generation and subsequent reaction of the dichlorocarbene radicals in our

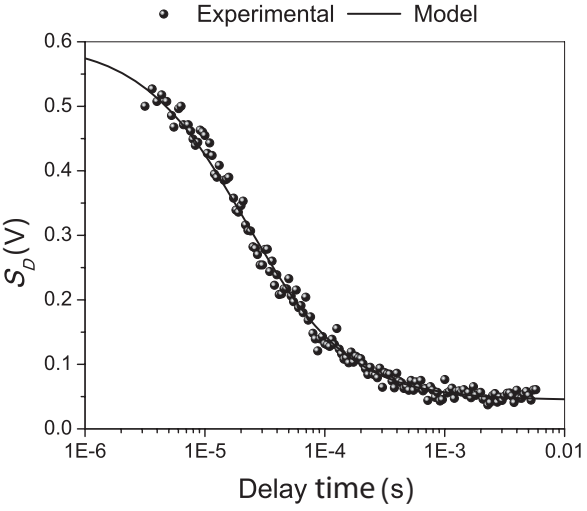

Figure 3 S_D dependence on the delay time between the dissociation and excitation lasers' pulses. Symbols: experimental data, line: data calculated with Eq. (10).

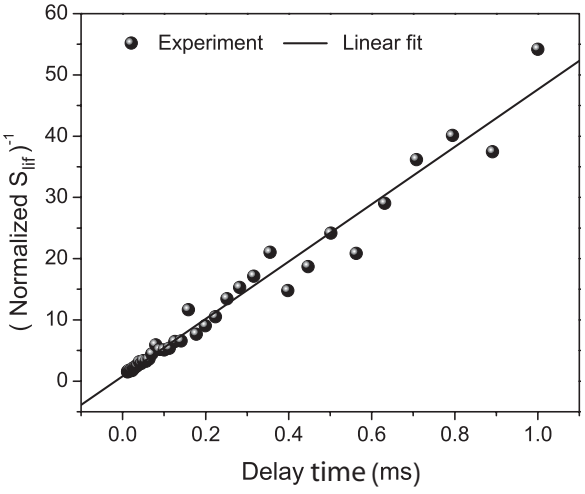

Figure 4 Delay time dependence of the inverse of the normalized LIF signal for an Ar pressure of 6 Torr and a fluence of 100 J cm^{-2}.

experimental conditions can be described by

$$CDCl_3 + nh\nu \rightarrow CCl_2 + DCl \quad (6)$$

$$CCl_2 + CCl_2 + M \xrightarrow{k_T} C_2Cl_4 + M \quad (7)$$

the time dependence of the CCl_2 radicals after the photolysis of $CDCl_3$ can be expressed by

$$\frac{d[CCl_2]}{dt} = -2k_T[CCl_2]^2 \quad (8)$$

where k_T is the rate constant of the termolecular reaction. The time dependence of the CCl_2 radicals concentration is obtained from the solution of Eq. (8):

$$[CCl_2](t) = \frac{[CCl_2]_0}{1 + 2k_T[CCl_2]_0 t} \quad (9)$$

Considering that the LIF signal is proportional to the radicals' concentration, the detected signal, S_D, will be given by

$$S_D(t) = S_{lif}(t) + S_b = \frac{q_i}{1 + \beta t} + S_b \quad (10)$$

where $\beta = 2k_T[CCl_2]_0$, q_i is proportional to the initial concentration of radicals, and S_b is the background signal in the absence of CCl_2 radicals. The coefficient q_i is a constant, which accounts for experimental factors such as the photomultiplier response, the fluorescence signal emitted in the observation solid angle, and the ratio of the number of radicals in the observation volume to the total number of radicals excited by the dye laser. The inverse value of β represents the mean lifetime of the radicals in the observation volume, τ, and depends on the rate constant of reaction and on the initial concentration of radicals. Equation (10) was used to fit the LIF signal maximum versus the delay time for the different Ar pressures with q_i, β, and S_b as the adjusting parameters. A typical example is shown in Fig. 3.

Also, Fig. 4 shows a plot of the delay time dependence of the inverse of the normalized LIF signal for an Ar pressure of 6 Torr and fluence of 100 J cm^{-2}. The experimental data are well described by a linear fit showing that the radicals disappearance follows a second-order kinetic due to the recombination reaction (7).

The initial concentration of radicals is an essential magnitude that directly affects the recombination rate, and, as it can be observed in Fig. 2, it depends on the irradiation fluence. This fact led us to study the dependence of the fluorescence intensity estimator $S_{lif}(t)$ of a mixture of 1 Torr $CDCl_3$ with 5 Torr Ar on the lasers pulses' delay time for two irradiation fluences, 15 and 100 J cm^{-2}. The experimental results of the normalized fluorescence intensity (symbols) and the values calculated with the help of Eq. (10) are shown in Fig. 5.

As can be observed, the radicals' mean lifetime at 100 J cm^{-2} is shorter than that at 15 J cm^{-2}. On the other hand, from Fig. 2 it results that 100 J cm^{-2} exceeds the fluence value required for $CDCl_3$ IRMPD saturation, whereas 15 J cm^{-2} lies below the saturation fluence level. The values of β for both fluences

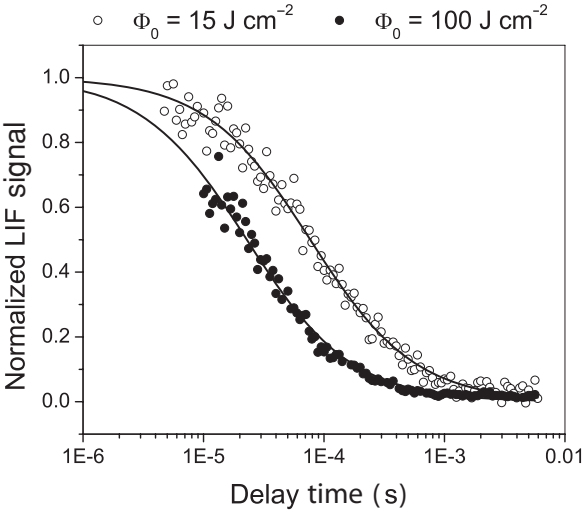

Figure 5 Delay time dependence of the normalized fluorescence intensity of a mixture of 1 Torr $CDCl_3$ and 5 Torr Ar for 15 and 100 J cm^{-2}.

were obtained from the curves fitted with Eq. (10). The resulting mean lifetime values of the radicals were $\tau\,(15) = (79.8 \pm 3{,}6)\ \mu s$ and $\tau\,(100) = (22.9 \pm 1.8)\ \mu s$, where the errors correspond to one standard deviation, and their ratio was

$$\tau(15)/\tau(100) = 3.5 \pm 0.3$$

Since the kinetic mechanism of the radicals disappearance is determined by reaction (7), this ratio must coincide with that of the radicals' concentration at 100 and 15 J cm^{-2}. The LIF signal values obtained from Fig. 2 at these fluences were

$$S_{\text{lif}}(15) = (1.1 \pm 0.2)\,V$$
$$S_{\text{lif}}(100) = (3.2 \pm 0.5)V$$

and therefore

$$S_{\text{lif}}(100)/S_{\text{lif}}(15) = (2.9 \pm 0.6)$$

Both results agree within experimental error supporting the statement that in our experimental conditions the CCl_2 radicals' disappearance is associated only to the recombination reaction to form C_2Cl_4, reaction (7). Therefore, for the experiments performed at 100 J cm^{-2}, the time dependence of S_{lif} was fitted with Eq. (10) assuming an initial concentration of CCl_2 radicals of 1 Torr since every $CDCl_3$ molecule in the observation volume was dissociated [22]. The pressure dependence of the recombination rate constant k_T was obtained from the fits of $S_{\text{lif}}(t)$ for the different Ar pressures.

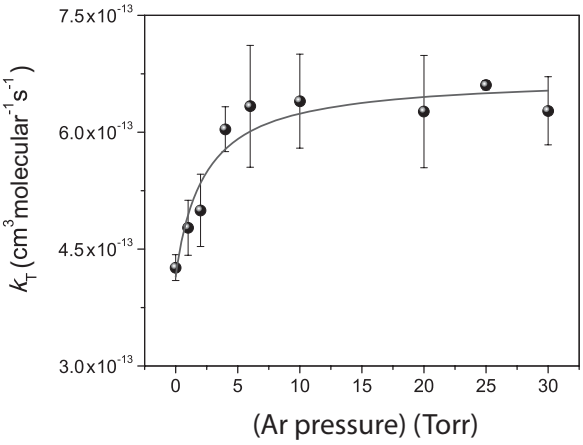

Figure 6 Ar pressure dependence of the rate constant of the CCl_2 radicals' recombination reaction. Symbols: experimental data, line: values calculated with Eq. (11).

The dependence of the CCl_2 radicals' recombination reaction rate constant, k_T, on Ar pressure is shown in Fig. 6. Values are the result of the average of five experiments, and error bars correspond to one standard deviation. It can be seen that k_T attains a saturation regime for Ar pressures larger than 5 Torr. This behavior is characteristic of termolecular reactions, which in the low-pressure regime behave as third order and in the high-pressure limit as second order. The termolecular reaction rate constant dependence on total pressure is given by

$$k_T = \frac{k_0([\text{Ar}] + \eta\text{M})}{1 + \frac{k_0}{k_\infty}([\text{Ar}] + \eta\text{M})} \qquad (11)$$

where k_0 and k_∞ are the low- and high-pressure limits. In obtaining Eq. (11), the termolecular reaction is considered as two successive bimolecular processes involving a reactive intermediate. The rate constant as expressed in (11) is obtained assuming a stationary state for the intermediate [24]. The collisions of the reactive intermediate, $C_2Cl_4^*$, with Ar were differentiated from those with other compounds M (mainly CCl_2 and DCl). The empirical parameter η added in the pressure factor takes into account the stabilization efficiency of the reactive intermediate $C_2Cl_4^*$ through collisions with CCl_2 and DCl relative to those with Ar.

The reaction rate constant values in the low- and high-pressure limit, k_0 and k_∞, respectively, resulted:

$$k_0 = (2.23 \pm 0.89) \times 10^{-29}\ \text{cm}^6\ \text{molecules}^{-2}\ \text{s}^{-1}$$
$$k_\infty = (6.73 \pm 0.23) \times 10^{-13}\ \text{cm}^3\ \text{molecules}^{-1}\ \text{s}^{-1}$$

where the errors correspond to one standard deviation.

The values of k_T shown in Fig. 6 determine a mean radical lifetime of 20–40 μs. In Eq. (8), we have neglected dilution effects caused by diffusion. Bialkowski et. al. [25] studied the mass transport rates of CF_2 radicals generated by laser-induced dissociation of CF_2HCl and C_2F_3Cl diluted in Ar and obtained a diffusion coefficient value of $D_{CF2} = 90$ cm^2 Torr s^{-1}. Assuming the same diffusion coefficient value for the CCl_2 radicals and defining the characteristic time for dilution as the time required for the radicals to travel a path comparable to the IR beam's radius at the focus, the mean lifetime of the radicals (≈20 μs) for an Ar pressure larger than 5 Torr would be less than the time required for dilution (>100 μs), so that the kinetics of the radicals disappearance would be dominated by the reaction. Although for Ar pressures lower than 5 Torr the mean lifetime of the radicals would be comparable to the estimated dilution time, we expect diffusion effects to be negligible in this pressure range since we obtained an increase in the rate constant of the reaction with pressure. Nevertheless since Cl atoms are heavier and larger than F atoms, we would expect that the diffusion coefficient of CCl_2 in Ar would be lower than that of CF_2 so that the conditions described above would be still less restrictive. These arguments are reinforced by the second-order decay of the radicals shown in Fig. 4.

Another important aspect of the present work is that the measurements were performed at room temperature. In the IRMPD of molecules, the radiation interacts resonantly with one of the species present in the sample whereas the other compounds act as a thermal bath. In our experiments, the bath consisted of Ar at room temperature. The final temperature of the products will be determined by the excess of energy attained above the threshold required for dissociation. Herman et al. [11] determined for the IRMPD of $CDCl_3$ through the DCl elimination channel a threshold energy of 63 kcal mol^{-1}. The excess of energy reached above this threshold will be distributed among the rotational and vibrational modes of the fragments, as well as in their translational energy distribution. In [11], the authors determined for the IRMPD products of $CDCl_3$ at 35 J cm^{-2} a mean translational energy of 2.8 kcal mol^{-1}, that is equivalent to the energy of an IR quanta (≈1000 cm^{-1}), showing that the $CDCl_3$ molecules are not highly excited above the dissociation threshold. Since 35 J cm^{-2} exceeds the value required to saturate the IRMPD of $CDCl_3$, we expect that the translational energy distribution of the fragments obtained in the experiments presented in this work at 100 J cm^{-2}, would not differ much from that of [11]. Given that the reaction process can be estimated to occur in about 100–1000 collisions, we can consider that the fragments obtained in the IRMPD of $CDCl_3$ would be thermalized before the recombination takes place.

The value of the factor η was obtained from the comparison of the experimental data with those calculated with Eq. (11) (Fig. 6). This value, $\eta = 1.52 \pm 0.67$, close to unity, indicates that collisions with CCl_2 and DCl would be as effective as collisions with Ar for the stabilization of the reactive intermediate $C_2Cl_4^*$ in the low-pressure regime.

On comparison with other experiments, Won and Bozzelli [15] have determined the high-pressure limit values of the rate constant for the association reaction of two CCl_2 radicals to form C_2Cl_4 in the temperature range of 800–1073 K. At 800 K, this value was 5.1×10^{-12} cm^3 molecules^{-1} s^{-1} whereas extrapolation to 300 K would result in 7.0×10^{-11} cm^3 molecules^{-1} s^{-1}. It is important to note that the authors inform that in the lower temperature range employed (848–953 K), their model overpredicts the concentration of C_2Cl_4. Later, Zhu and Bozzelli [20] reported revised high-pressure limit values of this rate constant in the temperature range of 300–2000 K calculated from complex mechanisms used to fit products' distributions from $CHCl_3$ pyrolysis using RRKM and QRRK rate theories. At 300 K, the value obtained was 6.0×10^{-12} cm^3 molecules^{-1} s^{-1}. This value results an order of magnitude higher than that obtained in a direct manner in this work.

On the other hand, the high-pressure limit value of the dichlorocarbene radicals' recombination reaction rate constant obtained in this work is in good agreement with the recombination reaction rate constants of other halocarbonated methylene radicals values obtained at room temperature in different pressure ranges and for different buffer gases reported by several authors [25–33]. Particularly, in [32] the laser flash-photolysis absorption technique was used to study the self-recombination reactions of CClF radicals as well as with CF_2 at 297 K. The derived high-pressure rate coefficients obtained $(1.2 \pm 0.2) \times 10^{-12}$ cm^3 molecules^{-1} s^{-1} and $(9 \pm 2) \times 10^{-13}$ cm^3 molecules^{-1} s^{-1}, respectively, are in good agreement within experimental error with the value obtained in this work.

To our knowledge, the low-pressure limit value obtained in this work would be the first value reported at 298 K. The only reported value in the literature is that of Kumaran el al. [18], which is valid in the temperature range 1280–1880 K. Extrapolation to 298 K results in 3.6×10^{-28} cm^6 molecules^{-2} s^{-1}, an order of magnitude higher than the value reported in this work. However, this extrapolation is not straightforward due to the temperature range in which the measurements were performed.

CONCLUSIONS

The LIF technique supported by FTIR spectrometry was used to determine the recombination reaction rate constant of CCl_2 radicals to form C_2Cl_4 in an Ar bath.

IRMPD of $CDCl_3$ with a TEA CO_2 laser was used to generate the CCl_2 radicals. The only dissociation pathway observed was the three-center DCl elimination consistent with previous studies.

The major products obtained determined by FTIR spectrometry were DCl and C_2Cl_4. The kinetics observed by the LIF technique is consistent with that of the recombination reaction of CCl_2 to form C_2Cl_4.

The low- and high-pressure limits of the rate constant of the CCl_2 radicals association reaction at 298 K were obtained in a direct manner, and the values resulted:

$$k_0 = (2.23 \pm 0.89) \times 10^{-29}\,\mathrm{cm^6\,molecules^{-2}\,s^{-1}}$$

$$k_\infty = (6.73 \pm 0.23) \times 10^{-13}\,\mathrm{cm^3\,molecules^{-1}\,s^{-1}}$$

To our knowledge, the low-pressure limit value obtained would be the first value reported at 298 K. The high-pressure limit value obtained results an order of magnitude lower than that calculated from complex mechanisms used to fit product distributions in a previous work of Zhu and Bozzelli [20]. It is consistent with the values obtained for other halocarbonated methylene radicals [25–33].

BIBLIOGRAPHY

1. Shen, Y. S.; Ku, Y. Water Res 1998, 32, 2669.
2. Martin, S. T. W.; Lee, A. T.; Hoffmann, M. R. Environ Sci Technol 1995, 29, 2567.
3. Choi, W.; Hoffmann, M. R. J Phys Chem 1996, 100, 2161–2169.
4. Choi, W.; Hoffmann, M. R. Environ Sci Technol 1997, 31, 89.
5. Intarajang, K.; Richardson, J. T. Appl Catal B: Environ 1999, 22, 27.
6. Coute, N.; Ortego, J. D.; Richardson, J. T.; Twigg, M. V. Appl Catal B: Environ 1998, 19, 175.
7. Taylor, P. H.; Lenoir, D. Sci Total Environ 2001, 269, 1–24.
8. Semeluk, G. P.; Bernstein, R. B. J Am Chem Soc 1954, 76, 3793–3796.
9. Semeluk, G. P.; Bernstein, R. B. J Am Chem Soc 1956, 79, 46–49.
10. Yano, T. Bull Chem Soc Jpn 1977, 50, 1272–1277.
11. Herman, I. P.; Magnotta, F.; Buss R. J.; Lee, Y. T. J Chem Phys 1983, 79, 1789–1794.
12. Chuang, S. C.; Bozzelli, J. W. Environ Sci Technol 1986, 20, 568–574.
13. Taylor, P. H.; Dellinger, B. Environ Sci Technol 1988, 22, 438–447.
14. Taylor, P. H.; Dellinger, B.; Tirey, D. A. Int J Chem Kinet 1991, 23, 1051–1074.
15. Won, Y. S.; Bozzelli, J. W. Combust Sci Technol 1992, 85, 345–373.
16. Miller, G. P.; Cundy, V. A.; Bozzelli, J. W. Combust Sci Technol 1994, 98, 123–136.
17. Kraft, M.; Stöckelmann, E.; Bockhorn, H. In Twenty-Sixth Symposium (International) on Combustion, The Combustion Institute, 1996; pp. 2431–2437.
18. Kumaran, S. S.; Su, M. C.; Lim, K. P.; Michael, J. V.; Klippenstein, S.; DiFelice, J.; Mudipalli, P. S.; Kiefer, J. H.; Dixon, D. A.; Peterson, K. A. J Phys Chem A 1997, 101, 8653–8661.
19. Wu, Y. P.; Won, Y. S. Combust Flame 2000, 122, 312–326.
20. Zhu, L.; Bozzelli, J. W. Int J Chem Kinet 2003, 35, 647–660.
21. Won, Y. S. J Ind Eng Chem 2007, 13, 400–405.
22. Gómez, N. D.; D'Accurso, V.; Codnia, J.; Manzano, F. A.; Azcárate, M. L. Appl Phys B 2012, 106, 921–926.
23. Gómez, N. D.; D'Accurso, V.; Codnia, J.; Manzano, F. A.; Azcárate, M. L. Anal AFA 2011, 23 (in press).
24. Benson, S. W. The Foundations of Chemical Kinetics; McGraw-Hill: New York, 1960; Chap. 12.
25. Bialkowski, S. E.; King, D. S.; Stephenson, J. C. J Chem Phys 1980, 72, 1156.
26. Chowdhury, P. K.; Pola, J.; Rao, K. V. S. R.; Mittal, J. P. Chem Phys Lett 1987, 142, 252.
27. Dalby, F. W. J Chem Phys 1964, 41, 2297.
28. Tyerman, W. J. R. J Chem Soc, Faraday Trans 1969, 65, 163.
29. Sharpe, S.; Hartnett, B.; Sethi, H. S.; Sethi, D. S. J Photochem 1987, 38, 1.
30. Sarkar, S. K.; Palit, D. K.; Rao, K. V. S. R.; Mittal, J. P. Chem Phys Lett 1986, 131, 303.
31. Chowdhury, P. K.; Rao, K. V. S. R.; Mittal, J. P. J Phys Chem 1988, 92, 102.
32. Caballero, N. B.; Castellano, E.; Cobos, C. J.; Croce, A. E.; Pino, G. A. Chem Phys 1999, 246, 157.
33. Meunier, H.; Purdy, J. R.; Thrush, B. A. J Chem Soc, Faraday Trans 2 1980, 76, 1304.